6th International Congress of Serbian Society of Mechanics
Mountain Tara, Serbia, June 19-21, 2017

IMPLICIT STRESS INTEGRATION OF THE ELASTIC-PLASTIC STRAIN HARDENING MODEL BASED ON MOHR-COULOMB

Dragan Rakić[1], Miroslav Živković[1], Milan Bojović[1]

[1] Faculty of Engineering
University of Kragujevac, Sestre Janjić 6, 34000 Kragujevac, Serbia
e-mail: drakic@kg.ac.rs

Abstract:

The paper presents implicit stress integration of the elastic-plastic strain hardening constitutive model with non-associative yield condition based on the Mohr-Coulomb model using incremental plasticity theory. Yield surface of the presented constitutive model is defined using material parameters whose interpretation and estimation is presented in the paper. Governing parameter method was used for solving of non-linear equation system. Implicit integration procedure of model constitutive relations is presented in details as well as the algorithm for its FEM implementation. Developed algorithm was implemented in the general-purpose finite element program PAK designed for static and dynamic, linear and non-linear analysis of the structures. Verification of the implemented algorithm is performed using test example.

Key words: Mohr-Coulomb, hardening, constitutive model, stress integration, FEM, PAK

1. Introduction

Stress integration represents calculation of stress change during an incremental step, corresponding to strain increments in the step. The essence of the incremental integration of inelastic constitutive relations is to trace the history of material deformation. The stress integration is an important ingredient in the overall finite element inelastic analysis of structures. It is crucial that the integration algorithm accurately reproduces the material behavior since the mechanical response of the entire structure is directly dependent on this accuracy. The algorithm should be also computationally efficient because the stress integration is performed to all integration points. For general applications, this computational procedure should be robust, providing reliable results under all possible loading conditions. This paper presents the computational procedure for implicit stress integration of the elastic-plastic strain hardening model based on Mohr-Coulomb [1, 2] using incremental plasticity method [3]. Integration steps of the constitutive relations were summarized in the form of algorithm and implemented into the program PAK. The implemented algorithm is verified by comparing the numerical results with the results of the shear test of soil.

2. Elastic-plastic constitutive matrix

Elastic-plastic constitutive models are described using elastic-plastic constitutive relations. In incremental plasticity theory, stress is directly proportional to strain up to reaching yield stress. After reaching yield stress, strain increment can be divided into elastic and plastic part [4]

$$d\mathbf{e} = d\mathbf{e}^E + d\mathbf{e}^P \tag{1}$$

Only elastic part of strain causes the stress change thus the stress increment can be formulated as

$$d\boldsymbol{\sigma} = \mathbf{C}^E d\mathbf{e}^E \tag{2}$$

where $\mathbf{C}^E$ is elastic constitutive matrix. Substituting (1) into (2), the following is obtained

$$d\boldsymbol{\sigma} = \mathbf{C}^E \left(d\mathbf{e} - d\mathbf{e}^P \right) \tag{3}$$

In the case of elastic-plastic constitutive models with hardening, yield function depends on the stress state and so does the internal parameter κ. Therefore, the increment of yield function change can be formulated as

$$f\left(\boldsymbol{\sigma}, \kappa\right) = 0 \quad \text{and} \quad d\frac{\partial f}{\partial \boldsymbol{\sigma}}^T d\boldsymbol{\sigma} + \frac{\partial f}{\partial \kappa}^T d\kappa = 0 \tag{4}$$

In incremental plasticity theory, it is necessary that the yield function is in every time step less or equal to zero (neutral loading condition).

Implicit stress integration implies the increment of plastic strain in the direction normal to the plastic potential surface, which can be formulated as

$$d\mathbf{e}^P = d\lambda \frac{\partial g\left(\boldsymbol{\sigma}, \kappa\right)}{\partial \boldsymbol{\sigma}} \tag{5}$$

where $d\lambda$ is positive scalar, which is to be calculated, and plastic potential function g is the function of the stress and internal parameter κ. Substituting the plastic strain increment (5) in (3) and using (4), can be written

$$df = \frac{\partial f}{\partial \boldsymbol{\sigma}}^T \left(\mathbf{C}^E d\mathbf{e} - d\lambda \mathbf{C}^E \frac{\partial g}{\partial \boldsymbol{\sigma}} \right) + d\lambda \frac{\partial f}{\partial \kappa}^T \frac{\partial \kappa}{\partial d\mathbf{e}^P} \frac{\partial g}{\partial \boldsymbol{\sigma}} = 0 \tag{6}$$

The last term in the equation (6) represents hardening modulus [5], where:

$$H = -\frac{\partial f}{\partial \kappa}^T \frac{\partial \kappa}{\partial d\mathbf{e}^P} \frac{\partial g}{\partial \boldsymbol{\sigma}} \tag{7}$$

so, equation (6) can be written as

$$df = \frac{\partial f}{\partial \boldsymbol{\sigma}}^T \left(\mathbf{C}^E d\mathbf{e} - d\lambda \mathbf{C}^E \frac{\partial g}{\partial \boldsymbol{\sigma}} \right) - d\lambda H = 0 \tag{8}$$

from where scalar $d\lambda$ can be calculated as

$$d\lambda = \frac{\frac{\partial f}{\partial \boldsymbol{\sigma}}^T \mathbf{C}^E}{H + \frac{\partial f}{\partial \boldsymbol{\sigma}}^T \mathbf{C}^E \frac{\partial g}{\partial \boldsymbol{\sigma}}} d\mathbf{e} \tag{9}$$

Finally, using scalar $d\lambda$ from (9), stress increment $d\boldsymbol{\sigma}$ can be obtained using equations (3) and (5)in the function of total strain increment

$$d\boldsymbol{\sigma} = \mathbf{C}^{EP} d\mathbf{e} \tag{10}$$

where term $\mathbf{C}^{EP}$ represents elastic-plastic constitutive matrix

$$\mathbf{C}^{EP} = \mathbf{C}^{E} - \frac{\mathbf{C}^{E}\dfrac{\partial g}{\partial \boldsymbol{\sigma}}\dfrac{\partial f}{\partial \boldsymbol{\sigma}}^{T}\mathbf{C}^{E}}{H + \dfrac{\partial f}{\partial \boldsymbol{\sigma}}^{T}\mathbf{C}^{E}\dfrac{\partial g}{\partial \boldsymbol{\sigma}}} \tag{11}$$

3. Stress integration of the elastic-plastic strain hardening model

Elastic-plastic strain hardening model based on Mohr-Coulomb [1] represents modification of the original Mohr-Coulomb material model [6]. Yield surface of this model can be expressed using stress invariants in the following form

$$f = \frac{I_1}{3}\sin\phi(\kappa) + \sqrt{J_{2D}}\left(\cos\theta - \frac{1}{\sqrt{3}}\sin\theta\sin\phi(\kappa)\right) - c(\kappa)\cos\phi(\kappa) \tag{12}$$

while plastic potential function in general case may have different forms (non-associative yield condition) and it is defined by following equation

$$g = \frac{I_1}{3}\sin\psi(\kappa) + \sqrt{J_{2D}}\left(\cos\theta - \frac{1}{\sqrt{3}}\sin\theta\sin\psi(\kappa)\right) \tag{13}$$

In equations (12) and (13), I_1 and J_{2D} represent first stress invariant and second deviatoric stress invariant, while θ is Lode's angle. Material model has a hardening feature because the model parameters $c(\kappa)$, $\phi(\kappa)$ and $\psi(\kappa)$ are the functions of the effective plastic strain [7, 8]. Effective plastic strain can be calculated using the following equation

$$\kappa = \bar{e}^{P} = \sum d\bar{e}^{P} \tag{14}$$

while the increment of the effective plastic strain can be calculated as

$$d\bar{e}^{P} = d\lambda\sqrt{\frac{2}{3}\frac{dg}{d\boldsymbol{\sigma}}^{T}\frac{dg}{d\boldsymbol{\sigma}}} \tag{15}$$

Yield function of the strain hardening model based on Mohr-Coulomb is a function of the effective plastic strain, so yield surface equation (12) can be written in following form

$$f = f\left(\boldsymbol{\sigma}, c(\kappa), \phi(\kappa)\right) \tag{16}$$

In case when stress point reaches yield surface, according to (4), increment of the yield function is equal to zero in any time step, so the following equation is fulfilled

$$df\left(\boldsymbol{\sigma}, c(\kappa), \phi(\kappa)\right) = 0 \tag{17}$$

Using equation (4), previous condition can be represented using chain rule as

$$df = \frac{\partial f}{\partial \boldsymbol{\sigma}}^{T} d\boldsymbol{\sigma} + \frac{\partial f}{\partial c(\kappa)}dc(\kappa) + \frac{\partial f}{\partial \phi(\kappa)}d\phi(\kappa) = 0 \tag{18}$$

or

$$\frac{\partial f}{\partial \boldsymbol{\sigma}}^{T} d\boldsymbol{\sigma} + \frac{\partial f}{\partial c\left(\bar{e}^{P}\right)}\frac{\partial c\left(\bar{e}^{P}\right)}{\partial \bar{e}^{P}}d\bar{e}^{P} + \frac{\partial f}{\partial \phi\left(\bar{e}^{P}\right)}\frac{\partial \phi\left(\bar{e}^{P}\right)}{\partial \bar{e}^{P}}d\bar{e}^{P} = 0 \tag{19}$$

Last two terms in consistency equation (19), according to (7), represent hardening of the material

$$-Hd\lambda = \frac{\partial f}{\partial c\left(\bar{e}^{P}\right)}\frac{\partial c\left(\bar{e}^{P}\right)}{\partial \bar{e}^{P}}d\bar{e}^{P} + \frac{\partial f}{\partial \phi\left(\bar{e}^{P}\right)}\frac{\partial \phi\left(\bar{e}^{P}\right)}{\partial \bar{e}^{P}}d\bar{e}^{P}, \tag{20}$$

where H represents hardening parameter [5]. Using (20), equation (19) can be written as:

$$\frac{\partial f}{\partial \boldsymbol{\sigma}}^T d\boldsymbol{\sigma} - H d\lambda = 0 \tag{21}$$

and using (15) to (21), hardening parameter H can be calculated as

$$H = -\left(\frac{\partial f}{\partial c\left(\bar{e}^P\right)} \frac{\partial c\left(\bar{e}^P\right)}{\partial \bar{e}^P} + \frac{\partial f}{\partial \phi\left(\bar{e}^P\right)} \frac{\partial \phi\left(\bar{e}^P\right)}{\partial \bar{e}^P} \right) \sqrt{\frac{2}{3} \frac{dg}{d\boldsymbol{\sigma}}^T \frac{dg}{d\boldsymbol{\sigma}}} \tag{22}$$

Substituting plastic strain increment (5) in (3) stress increment in time step can be written as

$$d\boldsymbol{\sigma} = \mathbf{C}^E d\mathbf{e} - d\lambda \mathbf{C}^E \frac{\partial g}{\partial \boldsymbol{\sigma}} \tag{23}$$

Multiplying equation (23) with $\left(\mathbf{C}^E\right)^{-1}$ total strain increment can be calculated by

$$d\mathbf{e} = \left(\mathbf{C}^E\right)^{-1} d\boldsymbol{\sigma} + d\lambda \frac{\partial g}{\partial \boldsymbol{\sigma}} \tag{24}$$

and multiplying with $\frac{\partial f}{\partial \boldsymbol{\sigma}}^T \mathbf{C}^E$, knowing that $\mathbf{C}^E \left(\mathbf{C}^E\right)^{-1} = \mathbf{I}$, where $\mathbf{I}$ represent identity matrix, (24) can be written

$$\frac{\partial f}{\partial \boldsymbol{\sigma}}^T \mathbf{C}^E d\mathbf{e} = \frac{\partial f}{\partial \boldsymbol{\sigma}}^T d\boldsymbol{\sigma} + \frac{\partial f}{\partial \boldsymbol{\sigma}}^T \mathbf{C}^E d\lambda \frac{\partial g}{\partial \boldsymbol{\sigma}} \tag{25}$$

Substituting (21) in (25) scalar $d\lambda$ can be calculated as

$$d\lambda = \frac{\frac{\partial f}{\partial \boldsymbol{\sigma}}^T \mathbf{C}^E}{H + \frac{\partial f}{\partial \boldsymbol{\sigma}}^T \mathbf{C}^E \frac{\partial g}{\partial \boldsymbol{\sigma}}} d\mathbf{e} \tag{26}$$

Substituting (26) in (5), plastic strain increment can be written in form

$$d\mathbf{e}^P = \frac{\mathbf{C}^E \frac{\partial g}{\partial \boldsymbol{\sigma}} \frac{\partial f}{\partial \boldsymbol{\sigma}}^T}{H + \frac{\partial f}{\partial \boldsymbol{\sigma}}^T \mathbf{C}^E \frac{\partial g}{\partial \boldsymbol{\sigma}}} d\mathbf{e} \tag{27}$$

Finally, substituting scalar $d\lambda$ from (26) in (23) the stress increment $d\boldsymbol{\sigma}$ (3) can be written as the function of total strain increment $d\mathbf{e}$ in form

$$d\boldsymbol{\sigma} = \mathbf{C}^E d\mathbf{e} - \frac{\mathbf{C}^E \frac{\partial g}{\partial \boldsymbol{\sigma}} \frac{\partial f}{\partial \boldsymbol{\sigma}}^T \mathbf{C}^E}{H + \frac{\partial f}{\partial \boldsymbol{\sigma}}^T \mathbf{C}^E \frac{\partial g}{\partial \boldsymbol{\sigma}}} d\mathbf{e} \tag{28}$$

or

$$d\boldsymbol{\sigma} = \left(\mathbf{C}^E - \frac{\mathbf{C}^E \frac{\partial g}{\partial \boldsymbol{\sigma}} \frac{\partial f}{\partial \boldsymbol{\sigma}}^T \mathbf{C}^E}{H + \frac{\partial f}{\partial \boldsymbol{\sigma}}^T \mathbf{C}^E \frac{\partial g}{\partial \boldsymbol{\sigma}}} \right) d\mathbf{e} \tag{29}$$

which implies

$$\mathbf{C}^{EP} = \mathbf{C}^{E} - \frac{\mathbf{C}^{E}\dfrac{\partial g}{\partial \boldsymbol{\sigma}}\dfrac{\partial f}{\partial \boldsymbol{\sigma}}^{T}\mathbf{C}^{E}}{H + \dfrac{\partial f}{\partial \boldsymbol{\sigma}}^{T}\mathbf{C}^{E}\dfrac{\partial g}{\partial \boldsymbol{\sigma}}} \tag{30}$$

Equation (30) represents elastic-plastic constitutive matrix.

3.1 Hardening formulation

The mobilized friction angle in material, according to [1, 9], can be written as

$$\phi\left(\bar{e}^{P}\right) = \sin^{-1}\left(2\frac{\sqrt{\bar{e}^{P}\bar{e}_{f}^{P}}}{\bar{e}^{P} + \bar{e}_{f}^{P}}\sin\left(\phi_{f}\right)\right) \tag{31}$$

where $\bar{e}_{f}^{P}$ represents effective plastic strain required to mobilize peak friction angle ϕ_{f}. The relationship (31) is shown graphically in Fig. 1.

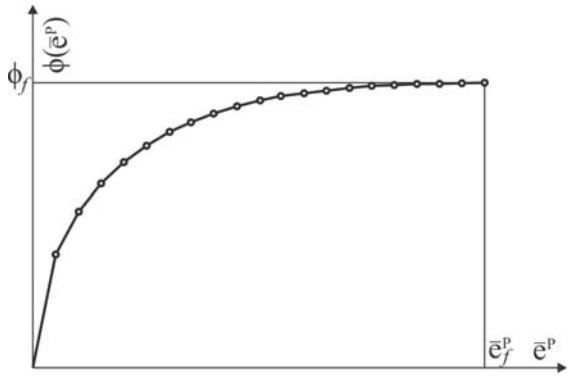

Fig. 1 Variation of internal friction angle with effective plastic strain

Cohesion hardening can be assumed to be linear [1] with respect to the effective plastic strain

$$c\left(\bar{e}^{P}\right) = c_{i} + h_{c}\bar{e}^{P} \tag{32}$$

where c_i represents initial cohesion, while h_c is cohesion hardening parameter. In order to limit the increase of the cohesion, the maximal value of the material parameter is specified as

$$c\left(\bar{e}^{P}\right) \le c_{f} \tag{33}$$

after that cohesion has a constant value. The dependence of the cohesion with respect to effective plastic strain is shown in Fig. 2.

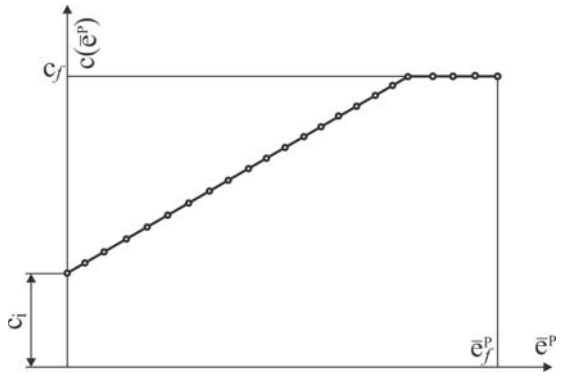

Fig. 2 Variation of cohesion with effective plastic strain

Dilatancy angle, as like as internal friction angle, is the function of the effective plastic strain and according to [1] can be expressed by equation

$$\psi\left(\bar{e}^P\right) = \sin^{-1}\left(\sin\psi_i + \left(\sin\psi_f - \sin\psi_i\right)\frac{\sin\phi\left(\bar{e}^P\right) - \sin\phi_i}{\sin\phi_f - \sin\phi_i}\right) \tag{34}$$

where ψ_i represents the initial dilation angle of the material, ϕ_i is initial friction angle, ψ_f is final dilation angle, while ϕ_f represents final friction angle. The dependence of the dilatancy angle with respect to effective plastic strain is shown in Fig. 3.

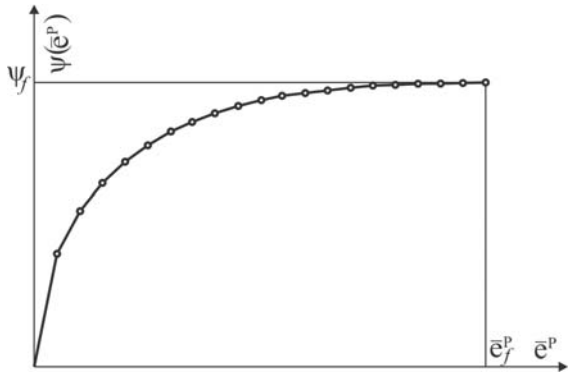

Fig. 3 Variation of dilatancy angle with effective plastic strain

3.2 Stress integration algorithm

Steps of implicit stress integration of strain hardening model based on Mohr-Coulomb are presented in the algorithm form [10] in the Table 1. Algorithm in the presented form was implemented in the program package PAK.

Table 1 Implicit stress integration algorithm of the strain hardening model

Known: ${}^{t+\Delta t}\mathbf{e}$, ${}^{t}\mathbf{e}$, ${}^{t}\boldsymbol{\sigma}$, ${}^{t}\mathbf{e}^{p}$, $\bar{e}^P$
A. Trial (elastic) solution:
$d\boldsymbol{\sigma} = \mathbf{C}^E d\mathbf{e}^E = \mathbf{C}^E\left({}^{t+\Delta t}\mathbf{e} - {}^{t}\mathbf{e}\right)$, ${}^{t+\Delta t}\boldsymbol{\sigma} = {}^{t}\boldsymbol{\sigma} + d\boldsymbol{\sigma}$
Stress invariants: I_1, J_{2D}, θ

Material parameters: $c\left(\bar{e}^P\right) = c_i + h_c \bar{e}^P$ for $c\left(\bar{e}^P\right) \le c_f$,

$$\phi\left(\bar{e}^P\right) = \sin^{-1}\left(2\frac{\sqrt{\bar{e}^P \bar{e}_f^P}}{\bar{e}^P + \bar{e}_f^P} \sin\left(\phi_f\right) \right),$$

$$\psi\left(\bar{e}^P\right) = \sin^{-1}\left(\sin\psi_i + \left(\sin\psi_f - \sin\psi_i\right) \frac{\sin\phi\left(\bar{e}^P\right) - \sin\phi_i}{\sin\phi_f - \sin\phi_i} \right)$$

Yield function: $$f = \frac{I_1}{3}\sin\phi\left(\bar{e}^P\right) + \sqrt{J_{2D}}\left(\cos\theta - \frac{1}{\sqrt{3}}\sin\theta\sin\phi\left(\bar{e}^P\right) \right) - c\left(\bar{e}^P\right)\cos\phi\left(\bar{e}^P\right)$$

Plastic potential function: $$g = \frac{I_1}{3}\sin\psi\left(\bar{e}^P\right) + \sqrt{J_{2D}}\left(\cos\theta - \frac{1}{\sqrt{3}}\sin\theta\sin\psi\left(\bar{e}^P\right) \right)$$

B. Yield condition check:

IF ($f < 0$) trial solution are elastic (GOTO **E**)

IF ($f \ge 0$) solution is elastic-plastic (CONTINUE)

$$\frac{\partial f}{\partial \boldsymbol{\sigma}} = \frac{\partial f}{\partial I_1}\frac{\partial I_1}{\partial \boldsymbol{\sigma}} + \frac{\partial f}{\partial J_{2D}}\frac{\partial J_{2D}}{\partial \boldsymbol{\sigma}} + \frac{\partial f}{\partial \theta}\frac{\partial \theta}{\partial \boldsymbol{\sigma}},$$

$$\frac{\partial g}{\partial \boldsymbol{\sigma}} = \frac{\partial g}{\partial I_1}\frac{\partial I_1}{\partial \boldsymbol{\sigma}} + \frac{\partial g}{\partial J_{2D}}\frac{\partial J_{2D}}{\partial \boldsymbol{\sigma}} + \frac{\partial g}{\partial \theta}\frac{\partial \theta}{\partial \boldsymbol{\sigma}},$$

$$\frac{\partial \theta}{\partial \boldsymbol{\sigma}} = \frac{\partial \theta}{\partial J_{2D}}\frac{\partial J_{2D}}{\partial \boldsymbol{\sigma}} + \frac{\partial \theta}{\partial J_{3D}}\frac{\partial J_{3D}}{\partial \boldsymbol{\sigma}}$$

$$d\lambda = \frac{\frac{\partial f}{\partial \boldsymbol{\sigma}}^{\mathbf{T}} \mathbf{C}^E d\mathbf{e}}{H + \frac{\partial f}{\partial \boldsymbol{\sigma}}^{\mathbf{T}} \mathbf{C}^E \frac{\partial g}{\partial \boldsymbol{\sigma}}}$$

C. Correction $d\lambda$ (local iterations): $d\mathbf{e}^P = d\lambda \frac{\partial g}{\partial \boldsymbol{\sigma}}$, $d\mathbf{e}^E = d\mathbf{e} - d\mathbf{e}^P$,

$$d\boldsymbol{\sigma} = \mathbf{C}^E d\mathbf{e}^E,\ {}^{t+\Delta t}\boldsymbol{\sigma} = {}^{t}\boldsymbol{\sigma} + d\boldsymbol{\sigma}$$

New stress invariants: I_1, J_{2D}, θ

Yield function: $$f = \frac{I_1}{3}\sin\phi\left(\bar{e}^P\right) + \sqrt{J_{2D}}\left(\cos\theta - \frac{1}{\sqrt{3}}\sin\theta\sin\phi\left(\bar{e}^P\right) \right) - c\left(\bar{e}^P\right)\cos\phi\left(\bar{e}^P\right)$$

D. IF ($ABS\left(f\right) \ge TOL$) go to **C** with new $d\lambda$:

$$d\bar{e}^P = d\lambda\sqrt{\frac{2}{3}\frac{dg}{d\boldsymbol{\sigma}}^T \frac{dg}{d\boldsymbol{\sigma}}},\ {}^{t+\Delta t}\bar{e}^P = {}^{t}\bar{e}^P + d\bar{e}^P,$$

$${}^{t+\Delta t}\mathbf{e}^P = {}^{t}\mathbf{e}^P + d\mathbf{e}^P$$

E. End: ${}^{t+\Delta t}\boldsymbol{\sigma}$, ${}^{t+\Delta t}\mathbf{e}^P$, $\bar{e}^P$

4. Model verification

4.1 Direct shear test

Verification of the developed algorithm for implicit stress integration of strain hardening model based on Mohr-Coulomb was performed through numerical simulation of direct shear test

in large scale. Due to its simplicity, direct shear test is often used for estimation of material model parameters. Therefore, numerical simulation of direct shear test is suitable for validation and verification of soil material models.

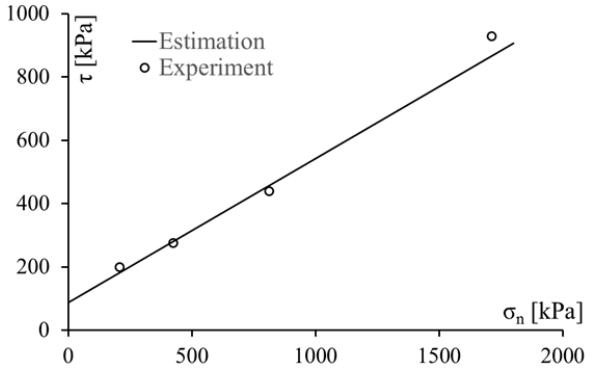

Fig. 4 Material parameter estimation

Results of experimental testing of supporting body material in Prvonek dam were used for estimation of material model parameters. Estimated material parameters are then used in numerical simulation of direct shear test. Analyzed sample represents rockfill of downstream slope L-1 of the Prvonek dam [11]. Since rockfill represents granular material type, its mechanical behavior can be described using strain hardening material model based on Mohr-Coulomb. Measured stress values during experiment are presented on Fig. 4. The same figure presents the yield surface of strain hardening model obtained through estimation, for final values of material model parameters ($\bar{e}_f^P$).

Values of estimated material parameters based on direct test experimental results and used in numerical simulation of direct shear test in large scale are shown in the Table 2.

Table 2 Estimated parameters of the strain hardening model based on Mohr-Coulomb

Parameter name	Sign	Value
Young's Modulus	E	$1x10^5$ kN/m^2
Poisson's Ratio	ν	0.3
Final cohesion	c_f	87.0 kN/m2
Final friction angle	ϕ_f	24.5°
Final effective plastic strain	$\bar{e}_f^P$	$3x10^{-2}$

FE model consisting of one finite element of unit dimensions was used for numerical simulation of direct shear test. Boundary conditions and loads used in the numerical simulation correspond to boundary conditions and loads in the testing device are presented on Fig. 5a. Load functions used in numerical simulation are presented on Fig. 5b.

During numerical simulation and experimental sample test, load was specified in two phases: in the first phase model was loaded up to specified stress level whereas in the second phase, normal stress keeps the constant value, during simultaneous applying of horizontal displacement which represents shear of the model. Shear displacement increases up to the failure with the monitoring of stress and strain changes.

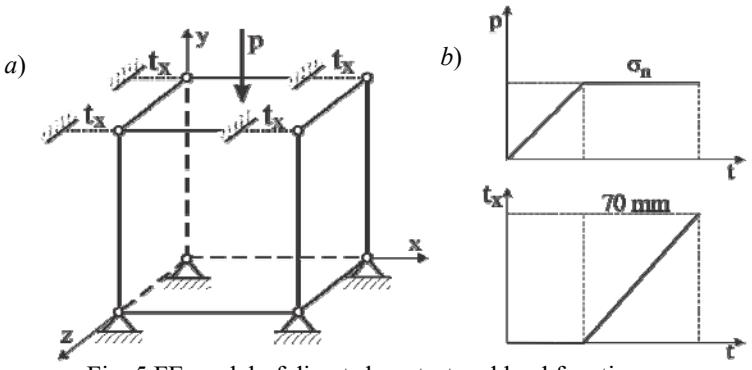

Fig. 5 FE model of direct shear test and load functions

Comparative values of shear stress obtained using Mohr-Coulomb model and strain hardening model based on Mohr-Coulomb for same material parameters are presented on Fig. 6. This figure presents the effect of model with hardening compared to classic Mohr-Coulomb material model.

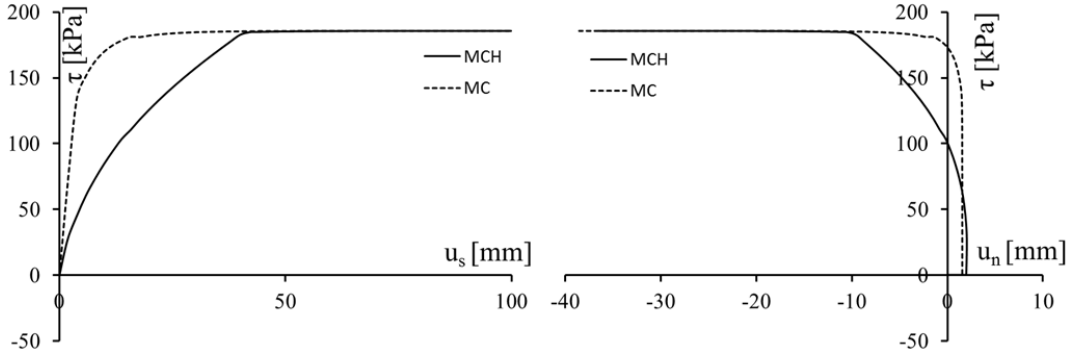

Fig. 6 Comparison of shear stress

Results of numerical simulation of direct shear test using the developed algorithm were compared to the results obtained using Mohr-Coulomb material model without hardening as well as to the results of experimental sample test. Comparative presentation of these results is presented on Fig. 7.

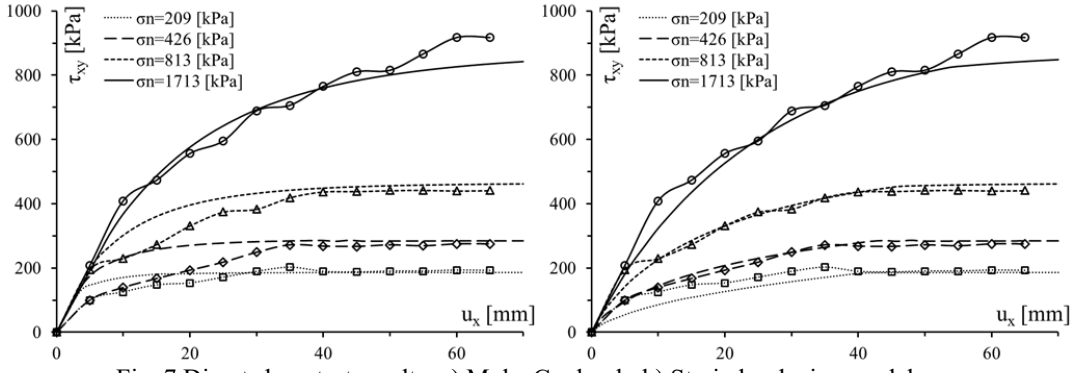

Fig. 7 Direct shear test results: a) Mohr-Coulomb, b) Strain hardening model

Analyzing the results presented on Fig. 7, it is noticed that both used material models provide matches with the experimental results for the high strain values. However, for the low strain values, strain hardening model based on Mohr-Coulomb provides better matches with the experimental results. These matches are the effect of the material hardening feature as the

function of effective plastic strain. Using of this material model provides more realistic modelling of the soil behavior. This proves that developed algorithm well describes mechanical behavior of analyzed sample of granular material. Therefore, it is proved that using of direct shear test results can be used for determination of material model parameters for using in numerical simulations of geotechnical problems.

5. Conclusions

This paper presents the implicit stress integration of strain hardening model with non-associative yield condition based on Mohr-Coulomb material model using the theory of incremental plasticity. Yield surface of the presented model was described through Mohr-Coulomb yield surface equation except that the model parameters in presented constitutive model are not constants but depend on the value of effective plastic strain. Developed material model was designed for numerical simulation of granular material mechanical behavior with and without cohesion. Steps of implicit stress integration of this material model are presented in the algorithm form which was implemented in the program PAK in the specified form. Governing parameter method was used for solving the equation system.

Developed algorithm was verified on the test example representing the simulation of direct shear test in large scale. Material parameters were obtained through estimation based on experimental results. Direct shear test using estimated material parameters was simulated in the repeated analysis. Numerical simulation results were compared to the experimental results as well as to the results obtained using Mohr-Coulomb model without hardening. The analysis of numerical simulation results indicates a good match with the experiment, using both material models. However, using of the presented material model with hardening provides better match for the small strain values. This is the consequence of model hardening feature so using of the presented material model with hardening provides more precise calibration of material parameters and therefore more precise numerical simulation of soil mechanical behavior.

Acknowledgements

The authors gratefully acknowledge partial support by Ministry of Science and Technology of the Republic of Serbia, grants TR37013 and TR32036.

References

[1] Vermeer P., Borst R., *Non-associated plasticity for soils, concrete and rock*, HERON, Vol. 29, No. 3, 1984.
[2] Rakić D., Živković M., *Stress integration of the Mohr-Coulomb material model using incremental plasticity theory*, Proceedings of Third Serbian (28th Yu) Congress on Theoretical and Applied Mechanics, Vlasina lake, Serbia, 2011.
[3] Bathe K. J., *Finite Element Procedures*, Massachusetts Institute of Technology, USA, 1996.
[4] Kojić M., Bathe K. J., *Inelastic Analysis of Solids and Structures*, 1 edition yp., Springer, 2004.
[5] Woods R., Rahim A., *CRISP2D Geotechnical finite element analysis software*, Technical reference manual, The CRISP Consortium Limited, 2007.
[6] Smith I., Griffiths V., *Programming the Finite Element Method*, John Wiley & Sons Ltd, England, 2004.
[7] Dounias G. T., Potts D. M., Vaughan P.R., *Finite element analysis of progressive failure: Two case studies*, Computers and Geotechnics, 155-175, 1988.

[8] Conte E., Silvestri F., Troncone A., *Stability analysis of slopes in soils with strain-softening behaviour*, Computers and Geotechnics, 710-722, 2010.
[9] Muhunthan B., Murugaiah S., *Numerical simulation of the performance of sand columns*, Washington State University, Department of Civil & Environmental Engineering, Pullman, 2006.
[10] Rakić D., *Development and application of material models for porous media in static and dynamic analysis of embankment dams*, PhD Thesis, University of Kragujevac, Faculty of Engineering, Kragujevac, 2014.
[11] Jaroslav Černi Institute for the Development of Water Resources, *Shear tests report on a large scale* (on Serbian), Jaroslav Černi Institute for the Development of Water Resources, Belgrade, 1995.